Published in final edited form as:
Chemosphere. 2011 October ; 85(3): 386–392. doi:10.1016/j.chemosphere.2011.07.004.

Crystal Structure and Density Functional Theory Studies of Toxic Quinone Metabolites of Polychlorinated Biphenyls

Yang Song[a,b], **Jyothirmai Ambati**[c], **Sean Parkin**[d], **Stephen E. Rankin**[c], **Larry W. Robertson**[b,e], and **Hans-Joachim Lehmler**[b,e,*]

[a]Key Laboratory on Luminescence and Real-Time Analysis (Ministry of Education), College of Pharmaceutical Sciences, Southwest University, Chong Qing, 400716, P.R. China

[b]Department of Occupational and Environmental Health, The University of Iowa, 100 UI Research Park, 221 IREH, Iowa City, IA 52242-5000, USA

[c]Department of Chemical and Materials Engineering, University of Kentucky, Lexington, KY 40506-13 0046, USA

[d]Department of Chemistry, University of Kentucky, Lexington, KY 40506-0055, USA

[e]Interdisciplinary Graduate Program in Human Toxicology, The University of Iowa, Iowa City, IA 52242-5000, USA.

Abstract

Lower chlorinated polychlorinated biphenyls (PCBs) are readily metabolized via hydroxylated metabolites to reactive PCB quinones. Although these PCB metabolites elicit biochemical changes by mechanisms involving cellular target molecules, such as the Aryl hydrocarbon receptor, and toxicity by interacting with enzymes like topoisomerases, only few PCB quinones have been synthesized and their conformational properties investigated. Similar to the parent compounds, knowledge of the three-dimensional structure of PCB quinones may therefore be important to assess their fate and risk. To address this gap in our knowledge, the gas phase molecular structure of a series of PCB quinones was predicted using HF/3-21G, B3LYP/6-31G** and UB3LYP/6-311G** calculations and compared to the respective solid state structure. All three methods overestimated the Cl-C bond length, but otherwise provided a reasonable approximation of the solid state bond angles and bond lengths. Overall, the UB3LYP/6-311G** level of theory yielded the best approximation of the molecular structure of PCB quinones in the solid state. Chlorine addition at the *ortho* position of both rings was found to increase the dihedral angle of the resulting quinone compound, which may have important implications for their interaction with cellular targets and, thus, their toxicity.

Keywords

Quinone; metabolite; solid state structure; dihedral angle; ground state energies

CORRESPONDING AUTHOR, Dr. H.-J. Lehmler, The University of Iowa, Department of Occupational and Environmental Health, University of Iowa Research Campus, 221 IREH, Iowa City, IA 52242-5000, Phone: (319) 335-4211, Fax: (319) 335-4290, hans-joachim-lehmler@uiowa.edu.

Introduction

PCBs are abundant and persistent environmental pollutants and were used as complex mixtures containing a large number of the possible 209 PCB congeners for a range of industrial application, including as coolants, lubricants, stabilizing additives in flexible PVC coatings of electrical wiring and electronic components (Hansen, 1999; Robertson and Hansen, 2001). They are still in use as dielectric fluids in transformers and capacitors in the United States. The production of PCBs was banned in the 1970s due to environmental and human health concerns; however, recent studies demonstrate that PCBs are formed inadvertently as byproducts of industrial processes and can be found as byproducts in paints (Hu and Hornbuckle). Furthermore, enviromental monitoring studies demonstrate that environmental PCB levels, for example in the Great Lakes, have only slowly decreased over the past decade (Hornbuckle et al., 2006). As a result, low level PCB exposures still represent a human health hazard that may be associated with multiple diseases, such as cancer, heart disease, developmental neurotoxicity and immunotoxicity in humans (Hansen, 1999; Robertson and Hansen, 2001).

In particular, lower chlorinated PCB congeners are readily metabolized by mammalian P450 enzymes to mono- (James, 2001; Letcher et al., 2000) and subsequently dihydroxylated PCB metabolites (Amaro et al., 1996; McLean et al., 1996). These dihydroxylated metabolites can undergo one electron reductions by both enzymatic and spontaneous reduction processes to form PCB semiquinone anion radicals (Song et al., 2008b; Venkatesha et al., 2008; Wangpradit et al., 2010) and, subsequently, be further oxidized to *ortho* or *para* PCB quinones (Amaro et al., 1996; Song et al., 2008b). *In vitro* studies have shown that some PCB quinones alter gene expression by interacting with the Aryl hydrocarbon receptor (AhR) (Machala et al., 2004). PCB quinones also may inactivate enzymes, like topoisomerases (Bender et al., 2007; Bender et al., 2006; Srinivasan et al., 2002). They readily react with glutathione (Amaro et al., 1996; Song et al., 2009; Srinivasan et al., 2002) and other cellular target molecules, including DNA (Amaro et al., 1996; Arif et al., 2003). PCB quinones can redox-cycle and, thus, contribute to the production of reactive oxygen species (McLean et al., 2000; Song et al., 2008b; Venkatesha et al., 2008). *In vivo* studies demonstrate that PCB quinones play a role in the carcinogenicity of lower chlorinated PCB by displaying initiating activity in the resistant hepatocyte model (Espandiari et al., 2004).

Despite the potential role of PCB quinones in the toxicity of lower chlorinated PCBs, few PCB quinones have been synthesized and little is known about their molecular structure. Considering the large number of PCB quinone metabolites that may be formed from the 209 possible PCB congeners, reliable approaches to predict their bond length and other structural parameters would aid in our understanding of their chemistry and, ultimately, toxicity. If accurate structure predictions can be made via computational chemistry, quantitative structure-activity relationships can be used to identify candidate compounds for toxicity generation from PCBs. Here we compare HF/3-21G, B3LYP/6-31G** and UB3LYP/6-311G** calculations to predict the molecular structure of six PCB quinones (Figure 1) in both the syn- and anti-like conformation and compare the results with the corresponding solid state data.

1. Experimental

1.1. Synthesis of PCB quinones

The structure and nomenclature of the six PCB quinones investigated is shown in Figure 1. They were synthesized as previously described (Amaro et al., 1996; Song et al., 2008a). Briefly, 2-(2-chloro-phenyl)-[1,4]benzoquinone (2'-Cl-2,5-Q), 2-(3-chloro-phenyl)-[1,4]benzoquinone (3'-Cl-2,5-Q), 2-(4-chloro-phenyl)-[1,4]benzoquinone (4'-Cl-2,5-Q), 2-

(2,5-dichloro-phenyl)-[1,4]benzoquinone (2',5'-Cl-2,5-Q) and 2-(3,4-dichloro-phenyl)-[1,4]benzoquinone (3',4'-Cl-2,5-Q) were synthesized from 1,4-benzoquinone and the corresponding chloroanilines using the Meerwein arylation. 2,5-Dichloro-3-(4-chloro-phenyl)-[1,4]benzoquinone (3,4',6-Cl-2,5-Q) was synthesized using the Suzuki cross-coupling reaction from 3-bromo-2,5-dichloro-1,4-dimethoxy-benzene and 4-chloro-phenylboronic acid, followed by oxidation with cerium ammonium nitrate. The analytical data for the PCB quinones were in agreement with the proposed structure. All PCB quinones were > 99% pure according to gas chromatographic analysis (based on relative peak area).

1.2. X-ray crystal structure analysis

Crystals of the PCB benzoquinones were obtained by slow crystallization from acetone. Diffraction data for crystals of 4'-Cl-2,5-Q, 2',5'-Cl-2,5-Q and 3',4'-Cl-2,5-Q were collected on a Nonius KappaCCD diffractometer system, but crystals of 2'-Cl-2,5-Q, 3'-Cl-2,5-Q and 3,4',6-Cl-2,5-Q proved too small for analysis on conventional small-molecule diffraction equipment. For these, diffraction data were collected using Cu*K*α x-rays on a specially configured hybrid small/macromolecule diffraction system based on the Bruker-Nonius X8 Proteum (Nonius FR-591 rotating anode x-ray generator, Bruker Helios graded multilayer optics, Nonius Kappa goniometer, Bruker SMART 6000 CCD detector). All data were collected at 90K using a CryoCool LN2 low temperature device from CryoIndustries of America.

For each crystal, initial unit cell parameters were obtained using either Denzo_SMN or APEX2 software (Bruker-Nonius, 2004). Final cell parameters were obtained either with Scalepack in DenzoSMN or SaintPlus in APEX2 (Bruker-Nonius, 2004) using spot positions from all data collection frames. Correction of Lorentz and polarization effects, data reduction, merging and an empirical absorption correction for each dataset were performed within either Denzo_SMN or APEX2 packages. The structures were solved by direct methods using SHELXS97 (Sheldrick, 2008) and refined by full-matrix least-squares against F^2 using SHELXL97 (Sheldrick, 2008). All non-hydrogen atoms in both structures were refined with anisotropic displacement parameters (ADPs).

Crystallographic data (excluding structure factors) for the structures in this paper have been deposited with the Cambridge Crystallographic Data Centre as supplementary publication nos. CCDC 806858 – 806863. Copies of the data can be obtained, free of charge, on application to CCDC, 12 Union Road, Cambridge CB2 1EZ, UK, (fax: +44-(0)1223-336033 or e-mail: deposit@ccdc.cam.ac.uk).

1.3. Calculations

The PCB quinone and semiquinone radical structures were built in ArgusLab 4.0 (Thompson). After the initial geometry optimization using the AM1 method in ArgusLab, these structures were re-optimized at HF/3-21G, B3LYP/6-31G** and UB3LYP/6-311G** levels of theory using Gaussian 03 (Frisch, 2004). These approaches have been used previously to predict the conformation, chemical properties and a range of other descriptors of a variety of environmental contaminants (Hu et al., 2005; Tuppurainen and Ruuskanen, 2003; Zhao et al., 2008). The unrestricted UB3LYP/6-311G** method was used as one of the methods for PCB quinones to facilitate comparison with the corresponding semiquinone radical structures in future studies. All of the Gaussian calculations were performed on an Intel Xeon based IBM HS21 blade cluster for isolated molecules in vacuum. Computed dihedral angles are the average of the four inter-ring dihedral angles of the optimized geometries. The bond length, angle and dihedral angle data sets were compared to the respective solid state data using linear regression analysis and the average relative percent difference (RPD). The RPD was calculated using the formula RPD = ($X_{\text{solid state}}$ −

$X_{calculated})/(1/2(X_{solid\ state} + X_{calculated})) \times 100$, where X is either the solid state or calculated bond length, bond angle or dihedral angle (Kostyniak et al., 2005).

2. Results and discussion

2.1. Solid state structure of PCB quinones

The solid state structure of only one PCB quinone, 2-(3,5-dichloro-phenyl)-[1,4]benzoquinone (3',5'-Cl-2,5-Q), has been reported previously (Lehmler et al., 2002b). Here we report the crystal structure of additional six PCB quinones (Figure 2). The three mono chlorinated PCB quinones (i.e., 2'-,3'- and 4'-Cl-2,5-Q) crystallized in an orthorhombic crystal system. The respective space groups were *Pca2₁* for 2'-Cl-2,5-Q and *P2₁2₁2₁* for 3'- and 4'-Cl-2,5-Q. In contrast, 2',5'-Cl-2,5-Q and 3,4',6-Cl-2,5-Q crystallized in the monoclinic space groups *P2₁/n* and *C2/c*, respectively. Similarly, we have reported previously that 3',5'-Cl-2,5-Q crystallizes in the monoclinic space group *P2₁/c* (Lehmler et al., 2002b). Only 3',4'-Cl-2,5-Q crystallized in the triclinic space group P $\bar{1}$.

Several structural parameters (i.e., Cl-C bond lengths, inter-ring C1-C1' bond length and dihedral angle between the phenyl and benzoquinone rings) are determinants of the three dimensional structure of PCB quinones and, thus, their toxicity. The solid state Cl-C bond length of all chlorine substituents in the phenyl ring ranged from 1.73 to 1.76 Å (Table 1). For comparison, the average Cl-C bond length of aromatic compounds and benzoquinones, as reported by the International Tables for Crystallography, is 1.739(10) Å (Allen et al., 1992). The inter-ring C1-C1' bond lengths ranged from 1.47 to 1.49 Å, which is also comparable to the average inter-ring bond length of 1.49(3) Å for non-*ortho* substituted biphenyls (Allen et al., 1992) (Table 1). Since all data collections were performed at low temperature, errors caused by libration (Schomaker and Trueblood, 1968) were expected to be small. For all six structures, the largest such correction was 0.002 Å, which is negligible compared to the standard uncertainties (typically 0.003 Å).

It is well established that the dihedral angles between the phenyl rings of PCBs play a role in their toxicity (Lehmler et al., 2002a; Shaikh et al., 2008; Vyas et al., 2006). Analogously, the dihedral angle between the phenyl and benzoquinone rings may influence the binding of PCB quinones to cellular targets. For example, Machala et al. have shown that 4'-Cl-2,5-Q and 3',4'-Cl-2,5-Q, but not 2'-Cl-2,5-Q, induce AhR-mediated activity (Machala et al., 2004). The dihedral angle of PCB quinones (and biphenyls in general) is determined by the balance of π-conjugation, which favors a planar conformation, and the repulsive interaction of *ortho* substituents. As a result, the solid state dihedral angle of the PCB quinones increased as expected with increasing number of *ortho* chlorine substituents. The four quinones with an unsymmetrical substitution pattern in the phenyl ring (i.e., 2'-Cl-2,5-Q, 3'-Cl-2,5-Q, 2',5'-Cl-2,5-Q and 3',4'-Cl-2,5-Q) adopted a syn-like conformation is the solid state. PCB quinones with one *ortho* chlorine substituent in the phenyl ring displayed the largest dihedral angles observed for this set of compounds, with dihedral angles of 67.8° and 71.8° for 2'-Cl-2,5-Q and 2',5'-Cl-2,5-Q, respectively (Table 2). Since 2'-Cl-2,5-Q and 2',5'-Cl-2,5-Q adopt a syn-like conformation in the solid state, with the *ortho* chlorine and oxygen substituents facing each other, these dihedral angles reflect the repulsive interaction of both substituents.

A dihedral angle of 57.0° was observed for 3,4',6-Cl-2,5-Q, the only PCB quinone with *ortho* chlorine and oxygen substituents in the benzoquinone ring. The three PCB quinones without *ortho* chlorine substituents displayed dihedral angles ranging from 37.3° to 45.7°. A comparable dihedral angle of 37.2° was also reported for 3',5'-Cl-2,5-Q (Lehmler et al., 2002b). For comparison, the solid state angle of 3,3',4,4'-tetrachlorobiphenyl (PCB 77), a potent AhR agonist, is 43.9° (Shaikh et al., 2008), and the gas phase dihedral angles of

biphenyl, 4-chlorobiphenyl and 4,4′-dichlorobiphenyl are approximately 44 to 45° (Almenningen et al., 1985a; Almenningen et al., 1985b). Thus, the crystal structure results indicate that PCB quinones can adopt a dihedral angle that may allow binding to AhR, despite the *ortho* carbonyl function of the benzoquinone system.

2.2. Quantum mechanical bond length predictions

The syn- and anti-like conformations of all six PCB quinones were optimized using the HF/3-21G, B3LYP/6-31G** and UB3LYP/6-311G** levels of theory. Figure 3 shows the corresponding conformation for 2'-Cl-2,5-Q as an example. Bond length were determined for the optimized structures in the syn- and, where appropriate, for the anti-like conformation. Overall, the predicted bond lengths obtained with all three approaches correlated well with the bond length from the crystal structure determinations ($R^2 > 0.99$). The average relative percent difference (RPD) (Kostyniak et al., 2005) of the solid state and calculated bond length ranged from 0.4% to 1.3%. Bond lengths calculated for the syn- and anti-like conformation were essentially identical. Overall, B3LYP/6-31G** and UB3LYP/6-311G** calculations yielded slightly better approximations of the solid state bond lengths than the HF/3-21G level of theory.

Selected bond lengths predicted from HF/3-21G, B3LYP/6-31G** and UB3LYP/6-311G** levels of theory for the six PCB quinones in the syn- and anti-like conformation are presented in Table 1. The Cl-C bonds determined with all three methods were longer compared to the solid state values, with the UB3LYP/6-311G** providing the closest approximately of the solid state bond length (Table 1). The Cl-C bond lengths of the corresponding parent PCBs, calculated using the B3LYP/6-31G** level of theory, ranged from 1.759 to 1.764 Å (Pan and Phillips, 2000; Pan et al., 2000), which is also longer compared to the solid state bond lengths of the corresponding PCB quinone (Table 1) and the average solid state Cl-C bond length of other aromatic compounds of 1.739(10)Å (Allen et al., 1992).

All three the methods predicted the observed inter-ring C1-C1' bond lengths accurately up to second decimal place (1.48 Å) (Table 1). This bond length is also comparable to the calculated C1-C1' bond length of PCBs, which ranged from 1.485 to 1.491 Å (Arulmozhiraja et al., 2002; Pan and Phillips, 2000; Pan et al., 2000). Thus, the computational methods provided a good estimation of the solid state C1-C1' bond length for both PCB quinones and their parent compounds. In the present study, the calculated HF/3-21G values (1.483 Å) remained unaffected by the chloro-substitution, whereas the B3LYP/6-31G** and UB3LYP/6-311G** C1-C1' bond lengths showed a systematic trend, with the C1-C1' bond length decreasing with the chlorine substituent moving away from it. A similar decrease of the C1-C1' bond length has been reported previously for PCBs and is a result of the weakening of the C1-C1' bond due to the larger dihedral angle in *ortho* substituted PCBs (Arulmozhiraja et al., 2002; Pan and Phillips, 2000; Pan et al., 2000). This substitution effect cannot be easily assessed experimentally due to accuracy limitations on coordinates for first row atoms in the crystal structure analysis. Overall, these results establish that both density functional theory (DFT) methods serve better in predicting the bond lengths trends of PCB quinones over the HF method using a minimal basis set. Both the restricted and unrestricted DFT methods made similar predictions and, with exception of Cl-C bond length predictions, the slight improvement in the basis sets from B3LYP/6-31G** to UB3LYP/6-311G** did not seem to be making any significant differences in the bond length predictions. Furthermore, the DFT methods allow the investigation of substitution effects that cannot be obtained experimentally.

2.3. Quantum mechanical bond angle predictions

Selected bond angles predicted from HF/3-21G, B3LYP/6-31G** and UB3LYP/6-311G** levels of theory (see Supporting Material) showed a slightly poorer correlation with the corresponding solid state bond angles in the syn- and anti-like conformation (R^2 = 0.69 to 0.96). The RPDs of the bond angles in the syn-like conformation compared to the solid state bond angles ranged from 0.2 to 1.0% for all three methods, which suggests that all three *in silico* methods are equally good at predicting the solid state bond angles of the PCB quinones RPDs ranging from 0.2 to 0.4% were observed when comparing bond angles in the syn- and anti-like conformation. The RPDs comparing the two different molecules A and B in the asymmetric unit of 2'-Cl-2,5-Q and 2',5'-Cl-2,5-Q with the corresponding calculated bond angles were larger for the more disordered molecule B. For 2',5'-Cl-2,5-Q, the RPD for this comparison increased from 0.3% for molecule A to 1.0% for molecule B at the B3LYP/6-31G** level of theory, which indicates that the presence of crystal packing effects causes a deformation of the PCB quinone molecules in the solid state.

2.4. Quantum mechanical dihedral angle predictions

The conformation and, more specifically, the dihedral angle are structural parameters that correlate with the affinity of PCBs and their metabolites for cellular targets, such as AhR, and, thus, their toxicity. Methods for predicting the dihedral angle of PCB quinones are therefore highly desirable, especially for PCB quinones that are not readily available and where the solid state structure is unknown. Both the HF/3-21G and UB3LYP/6-311G** method yielded dihedral angles for the syn-like conformation that are a reasonable estimate of the solid state structure values (Table 2), with an RPD of 6.6 and 6.9, respectively. In contrast, the B3LYP/6-31G** calculations of the syn-like conformation always underestimated the solid state dihedral angle, with an RPD of 10.3. The B3LYP/6-31G** values were also systematically lower than the dihedral angles obtained from the HF/3-21G and UB3LYP/6-311G** calculations.

All three methods predicted a similar difference in the dihedral angle of the syn- versus the anti-like conformation. Specifically, the dihedral angles for the anti-like conformation of the two PCB quinones with an *ortho* chlorine substituent (i.e., 2'-Cl-2,5-Q and 2',5'-Cl-2,5-Q) were approximately 12° smaller compared to the dihedral angle of the syn-like conformation. In contrast, all three methods predicted no effect of the *meta* chlorine substituent on the dihedral angle of 3'-Cl-2,5-Q and 3',4'-Cl-2,5-Q between the syn- and anti-like conformation.

Similar to the solid state values, the dihedral angles determined by the quantum mechanical methods display a clear effect of chlorine substitution on the dihedral angles in both the syn- and the anti-like conformation, with the dihedral angle decreasing as the chlorine moved from *ortho* to *meta* and *para* positions. For example, in the syn-like conformation the B3LYP/6-31G** calculations predicted dihedral angles of 53.5° to 64.9° and 36.7° to 38.4° for the PCB quinones with and without *ortho* chlorine substituents, respectively. A comparable effect of *ortho* chlorine substitution on the dihedral angles has also been reported for the corresponding parent PCBs using the same levels of theory (Arulmozhiraja et al., 2002; Pan and Phillips, 2000; Pan et al., 2000). For example, the B3LYP/6-31G** method predicts dihedral angles of 55.9° and 38.3° for 2- and 4-chlorobiphenyl, respectively (Pan and Phillips, 2000). The dihedral angles of the corresponding PCB quinones were comparable with 63.9° (2'-Cl-2,5-Q) and 37.0° (4'-Cl-2,5-Q), respectively (Table 2).

2.5. Ground state energies of PCB quinones

The ground state energies of the PCB quinones in the syn- and anti-like conformation were determined using the UB3LYP/6-311G** level of theory and are summarized in Table 3.

Overall, the energy differences between both conformations are minimal and range from 0.2 to 0.8 kJ mol^{-1}. In the case of *ortho* chlorinated PCB quinones, the syn-like conformation is energetically more favorable, whereas the anti-like conformation is energetically more favorable for PCB quinones with *meta* substituents. Arulmozhiraja et al. showed analogously that the ground state energies between the syn-and anti-like conformation of PCB congeners with two *ortho* chlorine substituents differ only slightly, with the anti-like conformation being 2 kJ mol^{-1} less stable.

3. Conclusions

HF/3-21G, B3LYP/6-31G** and UB3LYP/6-311G** calculations of isolated PCB quinone molecules in vacuum provided a reasonable approximation of their molecular structure in the solid state. All three theoretical methods predicted the solid state C1-C1' bond lengths accurately up to two decimal places, but in particular the HF/3-21G method overestimated the Cl-C bond length. The B3LYP/6-31G** and UB3LYP/6-311G** methods also showed a systematic effect of chlorine substitution on the length of the inter-ring C1-C1' bond, which was not apparent from the HF/3-21G calculations. While the bond angles determined with all three methods were comparable, the dihedral angles of the two ring systems were best predicted using HF/3-21G and UB3LYP/6-311G** calculations. Overall, the present study demonstrates that the UB3LYP/6-311G** level of theory offers the best approximation of the molecular structure of PCB quinones in the solid state, thus allowing reasonable structure predictions of PCB quinones of interest for toxicological studies. These structure predictions will aid in future quantitative studies of structure-activity relationships with cellular target molecules and, ultimately, contribute to our understanding of the risk associated with exposures to lower chlorinated PCBs and their metabolites.

Supplementary Material

Refer to Web version on PubMed Central for supplementary material.

Acknowledgments

We acknowledge the High Performance Computing Center at University of Kentucky for use of their facility for the Gaussian calculations. This research was supported by grants ES05605, ES013661 and ES017425 from the National Institute of Environmental Health Sciences (HJL and LWR) and MRI grant #0319176 (SP) from the National Science Foundation. The content is solely the responsibility of the authors and does not necessarily represent the official views of the National Institute of Environmental Health Sciences, National Institutes of Health, or the National Science Foundation.

References

Allen, FH.; Kennard, O.; Watson, DG.; Brammer, L.; Orpen, AG.; Taylor, R. Typical interatomic distances: organic compounds. In: Wilson, AJC., editor. International Tables for Crystallography. Vol. Vol. C. Dordrecht: Kluwer Academic Publishers; 1992. p. 685-706.

Almenningen A, Bastiansen O, Fernholt L, Cyvin BN, Cyvin SJ, Samdal S. Structure and barrier of internal rotation of biphenyl derivatives in the gaseous state : Part 1. The molecular structure and normal coordinate analysis of normal biphenyl and perdeuterated biphenyl. J. Mol. Struct. 1985a; 128:59–76.

Almenningen A, Bastlansen O, Gundersen S, Samdal S, Skancke A. Structure and barrier of internal rotation of biphenyl derivatives in the gaseous state : Part 3. Structure of 4-fluoro-, 4,4' -difluoro-, 4-chloro - and 4,4'-dichlorobiphenyl. J. Mol. Struct. 1985b; 128:95–114.

Amaro AR, Oakley GG, Bauer U, Spielmann HP, Robertson LW. Metabolic activation of PCBs to quinones: Reactivity toward nitrogen and sulfur nucleophiles and influence of superoxide dismutase. Chem. Res. Toxicol. 1996; 9:623–629. [PubMed: 8728508]

Arif JM, Lehmler H-J, Robertson LW, Gupta RC. Interaction of benzoquinone- and hydroquinone-derivatives of lower chlorinated biphenyls with DNA and nucleotides in vitro. Chem.-Biol. Interact. 2003; 142:307–316. [PubMed: 12453668]

Arulmozhiraja S, Fujii T, Morita M. Density functional theory studies on radical ions of selected polychlorinated biphenyls. J. Phys. Chem. A. 2002; 106:10590–10595.

Bender RP, Ham A-JL, Osheroff N. Quinone-induced enhancement of DNA cleavage by human topoisomerase IIa: Adduction of cysteine residues 392 and 405. Biochemistry. 2007; 46:2856–2864. [PubMed: 17298034]

Bender RP, Lehmler HJ, Robertson LW, Ludewig G, Osheroff N. Polychlorinated biphenyl quinone metabolites poison human topoisomerase IIa: Altering enzyme function by blocking the N-terminal protein gate. Biochem. 2006; 45:10140–10152. [PubMed: 16906772]

Bruker-Nonius. APEX2: Programs for data collection and reduction. Madison, WI, USA: Bruker-Nonius AXS; 2004.

Espandiari P, Glauert HP, Lehmler H-J, Lee EY, Srinivasan C, Robertson LW. Initiating activity of 4-chlorobiphenyl metabolites in the resistant hepatocyte model. Toxicol. Sci. 2004; 79:41–46. [PubMed: 14976334]

Frisch, MJTGW.; Schlegel, HB.; Scuseria, GE.; Robb, MA.; Cheeseman, JR.; Montgomery, JA., Jr; TV; Kudin, KN.; Burant, JC.; Millam, JM.; Iyengar, SS.; Tomasi, J.; Barone, V.; Mennucci, B.; Cossi, M.; Scalmani, G.; Rega, N.; Petersson, GA.; Nakatsuji, H.; Hada, M.; Ehara, M.; Toyota, K.; Fukuda, R.; Hasegawa, J.; Ishida, M.; Nakajima, T.; Honda, Y.; Kitao, O.; Nakai, H.; Klene, M.; Li, X.; Knox, JE.; Hratchian, HP.; Cross, JB.; Bakken, V.; Adamo, C.; Jaramillo, J.; Gomperts, R.; Stratmann, RE.; Yazyev, O.; Austin, AJ.; Cammi, R.; Pomelli, C.; Ochterski, JW.; Ayala, PY.; Morokuma, K.; Voth, GA.; Salvador, P.; Dannenberg, JJ.; Zakrzewski, VG.; Dapprich, S.; Daniels, AD.; Strain, MC.; Farkas, O.; Malick, DK.; Rabuck, AD.; Raghavachari, K.; Foresman, JB.; Ortiz, JV.; Cui, Q.; Baboul, AG.; Clifford, S.; Cioslowski, J.; Stefanov, BB.; Liu, G.; Liashenko, A.; Piskorz, P.; Komaromi, I.; Martin, RL.; Fox, DJ.; Keith, T.; Al-Laham, MA.; Peng, CY.; Nanayakkara, A.; Challacombe, M.; Gill, PMW.; Johnson, B.; Chen, W.; Wong, MW.; Gonzalez, C.; Pople, JA. Gaussian 03. Wallingford, CT: Gaussian, Inc.; 2004.

Hansen, LG. The *ortho* side of PCBs: Occurrence and disposition. Boston: Kluwer Academic Publishers; 1999.

Hornbuckle, KC.; Carlson, DL.; Swackhamer, DL.; Baker, JE.; Eisenreich, SJ. Polychlorinated Biphenyls in the Great Lakes. In: Hites, R., editor. The Handbook of Environmental Chemistry, j: Persistent Organic Pollutants in the Great Lakes. Vol. Vol. 5. Berlin, Heidelberg: Springer Verlag; 2006. p. 13-70.

Hu D, Hornbuckle KC. Inadvertent polychlorinated biphenyls in commercial paint pigments. Environ. Sci. Technol. 2010; 44:2822–2827. [PubMed: 19957996]

Hu J, Eriksson L, Bergman A, Kolehmainen E, Knuutinen J, Suontamo R, Wei X. Molecular orbital studies on brominated diphenyl ethers. Part I-conformational properties. Chemosphere. 2005; 59:1033–1041. [PubMed: 15823337]

James, MO. Polychlorinated Biphenyls: Metabolism and metabolites. In: Robertson, LW.; Hansen, L., editors. Proceedings of the PCB Workshop: Recent Advances in the Environmental Toxicology and Health Effects of PCBs. Lexington: University Press of Kentucky; 2001. p. 35-46.

Kostyniak PJ, Hansen LG, Widholm JJ, Fitzpatrick RD, Olson JR, Helferich JL, Kim KH, Sable HJK, Seegal RF, Pessah IN, Schantz SL. Formulation and characterization of an experimental PCB mixture designed to mimic human exposure from contaminated fish. Toxicol. Sci. 2005; 88:400–411. [PubMed: 16177234]

Lehmler H-J, Parkin S, Robertson LW. The three-dimensional structure of 3,3',5'-trichloro-4-methoxybiphenyl, a "coplanar" polychlorinated biphenyl (PCB) derivative. Chemosphere. 2002a; 46:485–488. [PubMed: 11829405]

Lehmler HJ, Robertson LW, Parkin S. 2-(3,5-Dichlorophenyl)-1,4-benzoquinone. Acta Cryst. 2002b; E58:o366–o367.

Letcher, RJ.; Klasson-Wehler, E.; Bergman, A. Methyl sulfone and hydroxylated metabolites of polychlorinated biphenyls. In: Paasivirta, J., editor. The handbook of environmental chemistry Vol. 3 Part K. New types of persistent halogenated compounds. Berlin Heidelberg: Springer Verlag; 2000. p. 315-359.

Machala M, Blaha L, Lehmler H-J, Pliskova M, Majkova Z, Kapplova P, Sovadinova I, Vondracek J, Malmberg T, Robertson LW. Toxicity of hydroxylated and quinoid PCB metabolites: Inhibition of gap junctional intercellular communication and activation of aryl hydrocarbon and estrogen receptors in hepatic and mammary cells. Chem. Res. Toxicol. 2004; 17:340–347. [PubMed: 15025504]

McLean MR, Bauer U, Amaro AR, Robertson LW. Identification of catechol and hydroquinone metabolites of 4-monochlorobiphenyl. Chem. Res. Toxicol. 1996; 9:158–164. [PubMed: 8924585]

McLean MR, Twaroski TP, Robertson LW. Redox cycling of 2-(x'-mono, -di, -trichlorophenyl)-1,4-benzoquinones, oxidation products of polychlorinated biphenyls. Arch. Biochem. Biophys. 2000; 376:449–455. [PubMed: 10775433]

Pan D, Phillips DL. Investigation of the effects of substitution position on the radical anions of chlorobiphenyls. Chem. Phys. Lett. 2000; 318:214–221.

Pan D, Shoute LCT, Phillips DL. Time-resolved resonance Raman and density functional study of the radical cations of chlorobiphenyls. Chem. Phys. Lett. 2000; 316:395–403.

Robertson, LW.; Hansen, LG. Recent advances in the environmental toxicology and health effects of PCBs. Lexington: University Press of Kentucky; 2001.

Schomaker V, Trueblood KN. Rigid-body motion of molecules in crystals. Acta Crystallogr. 1968; B24:63–76.

Shaikh NS, Parkin S, Luthe G, Lehmler H-J. The three-dimensional structure of 3,3',4,4'-tetrachlorobiphenyl, a dioxin-like polychlorinated biphenyl (PCB). Chemosphere. 2008; 70:1694–1698. [PubMed: 17723240]

Sheldrick GM. A short history of SHELX. Acta Cryst. 2008; A64:112–122.

Song Y, Buettner GR, Parkin S, Wagner BA, Robertson LW, Lehmler H-J. Chlorination increases the persistence of semiquinone free radicals derived from polychlorinated biphenyl hydroquinones and quinones. J. Org. Chem. 2008a; 73:8296–8304. [PubMed: 18839991]

Song Y, Wagner BA, Lehmler H-J, Buettner GR. Semiquinone radicals from oxygenated polychlorinated biphenyls: Electron paramagnetic resonance studies. Chem. Res. Toxicol. 2008b; 21:1359–1367. [PubMed: 18549251]

Song Y, Wagner BA, Witmer JR, Lehmler H-J, Buettner GR. Nonenzymatic displacement of chlorine and formation of free radicals upon the reaction of glutathione with PCB quinones. Proc. Natl. Acad. Sci. U.S.A. 2009; 106:9725–9730. [PubMed: 19497881]

Srinivasan A, Robertson LW, Ludewig G. Sulfhydryl Binding and Topoisomerase Inhibition by PCB Metabolites. Chemical Research in Toxicology. 2002; 15:497–505. [PubMed: 11952335]

Thompson, MA. ArgusLab 4.0.1 (www.arguslab.com). Seattle, WA: Planaria Software LLC;

Tuppurainen K, Ruuskanen J. NMR and molecular modeling in environmental chemistry: prediction of 13C chemical shifts in selected C10-chloroterpenes employing DFT/GIAO theory. Chemosphere. 2003; 50:603–609. [PubMed: 12685736]

Venkatesha VA, Venkataraman S, Sarsour EH, Kalen AL, Buettner GR, Robertson LW, Lehmler H-J, Goswami PC. Catalase ameliorates polychlorinated biphenyl-induced cytotoxicity in nonmalignant human breast epithelial cells. Free Radic. Biol. Med. 2008; 45:1094–1102. [PubMed: 18691649]

Vyas SM, Parkin S, Lehmler HJ. 2,2',3,4,4',5,5'-Heptachlorobiphenyl (PCB 180). Acta Cryst. E. 2006; E62:o2905–o2906.

Wangpradit O, Moman E, Nolan KB, Buettner GR, Robertson LW, Luthe G. Observation of an unusual electronically distorted semiquinone radical of PCB metabolites in the active site of prostaglandin H synthase-2. Chemosphere. 2010; 81:1501–1508. [PubMed: 20843536]

Zhao Y-Y, Tao F-M, Zeng EY. Theoretical study on the chemical properties of polybrominated diphenyl ethers. Chemosphere. 2008; 70:901–907. [PubMed: 17707458]

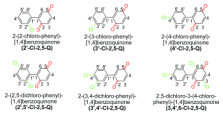

Figure 1.
Chemical structures, numbering scheme and nomenclature of PCB quinones.

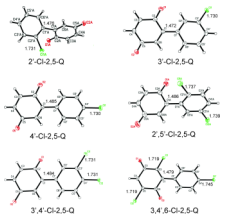

Figure 2.
Representative solid state molecular structures of PCB quinones showing selected bond lengths (Å) (see also Supporting Material, Figure S1 and S2). Displacement ellipsoids are drawn at the 50% probability level.

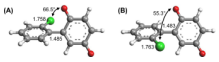

Figure 3.
Molecular structure of 2'-Cl-2,5-Q in the (A) syn- and (B) anti-like conformation as determined from the UB3LYP/6-311G** level of theory. The Cl-C and C1-C1' bond lengths (Å) and the dihedral angles are shown for both conformations.

Chemosphere. Author manuscript; available in PMC 2012 October 1.

Table 1

C1-C and C1-C1' inter-ring bond lengths calculated from HF/3-21G, B3LYP/6-31G**, UB3LYP/6-311G** levels of theory for PCB quinones in the syn- and anti-like conformation compared with solid state values.[1]

PCB Quinone	C1-C Bond Length (Å)							C1-C1' Inter-ring Bond Length (Å)						
	Solid State	HF/3-21G		B3LYP/6-31G**		UB3LYP/6-311G**		Solid State	HF/3-21G		B3LYP/6-31G**		UB3LYP/6-311G**	
		syn	anti	syn	anti	syn	anti		syn	anti	syn	anti	syn	anti
2'-C1-2,5-Q	1.731[A] 1.734[B]	1.815	1.820	1.758	1.763	1.758	1.763	1.476	1.483	1.483	1.485	1.485	1.485	1.483
3'-C1-2,5-Q	1.730	1.817	1.817	1.759	1.760	1.760	1.759	1.472	1.483	1.483	1.482	1.482	1.480	1.480
4'-C1-2,5-Q	1.730	1.816		1.756		1.757		1.485	1.483		1.478		1.478	
2',5'-C1-2,5-Q[#]	1.737 1.739	1.809 1.811	1.815 1.811	1.755 1.756	1.759 1.755	1.754 1.756	1.759 1.755	1.486	1.484	1.483	1.486	1.485	1.485	1.484
3',4'-C1-2,5-Q[$]	1.731 1.731	1.801 1.799	1.801 1.799	1.746 1.743	1.746 1.743	1.747 1.744	1.747 1.744	1.484	1.482	1.483	1.481	1.481	1.479	1.479
3,4',6-C1-2,5-Q[*]	1.719 1.745 1.719	1.813 1.789 1.792		1.755 1.732 1.737		1.732 1.756 1.736		1.479	1.483		1.483		1.482	

[1] See the supporting material for an extensive list of other bond length.

[A,B] Molecule A or B in the asymmetric unit.

The C1-C bond lengths are listed in the following order:

[#] C1-C2' and C1-C5',

[$] C1-C3' and C1-C4', and

[*] C1-C3, C1-C4', and C1-C6.

Chemosphere. Author manuscript; available in PMC 2012 October 1.

Table 2

Dihedral angle averages calculated from HF/3-21G, B3LYP/6-31G**, UB3LYP/6-311G** levels of theory for PCB quinones compared with solid state values.[1]

PCB Quinone	Dihedral Angle Average (°)						
	Solid State	HF/3-21G		B3LYP/6-31G**		UB3LYP/6-311G**	
		syn	anti	syn	anti	syn	anti
2'-C1-2,5-Q	67.8	73.1	61.5	63.9	52.5	66.5	55.3
3'-C1-2,5-Q	45.7	43.7	44.2	38.4	38.5	40.1	40.2
4'-C1-2,5-Q	45.5	43.8		37.0		38.7	
2',5'-C1-2,5-Q	71.8	73.1	61.4	64.9	52.8	67.6	55.4
3',4'-C1-2,5-Q	37.3	42.9	42.8	36.7	36.7	38.3	39.2
3,4',6-C1-2,5-Q	57.0	61.8		53.5		56.0	

[1] The *in silico* dihedral angles are the average of the four dihedral angles involving the C1-C1' bond between the benzene and the quinone rings.

Table 3

Ground state energies calculated at the UB3LYP/6-311G** level of theory for PCB quinones in the syn- and anti-like conformations.

PCB Quinone	Ground State energy (10^6 kJ/mol)		Difference in ground state energies (kJ/mol)
	syn	anti	syn - anti
2'-C1-2,5-Q	−2.82	−2.82	−0.6
3'-C1-2,5-Q	−2.82	−2.82	0.2
4'-C1-2,5-Q	−2.82		
2',5'-C1-2,5-Q	−4.02	−4.02	−0.8
3',4'-C1-2,5-Q	−4.02	−4.02	0.3
3,4',6-C1-2,5-Q	−5.23		